ANALYTICAL STUDY

Introduction

Various parameters affect structural response under seismic loading. To study the effect of their parameters, this research analyzes a series totally forty-two of reinforced concrete bridge pier models subjected to constant axial loads and lateral cyclic loading by controlling the displacement. The parameters of the study investigated were as follow: 1) tie reinforcement ratios 2) shear span ratio 3) level of axial force and eccentricity and 4) vertical reinforcement ratio.

Analytical Model Specimens

The analyzed reinforced concrete specimens are described in Table 5.1. For the symbol and specimen name in the first column, the first letter describes the amount of tie reinforcement ratio: H, M and L for high medium and low ratio. The second letter describes the levels of axial force index: H, M and L for high medium and low axial force levels. The two digits describe the shear span ratios and vertical reinforcement ratio.

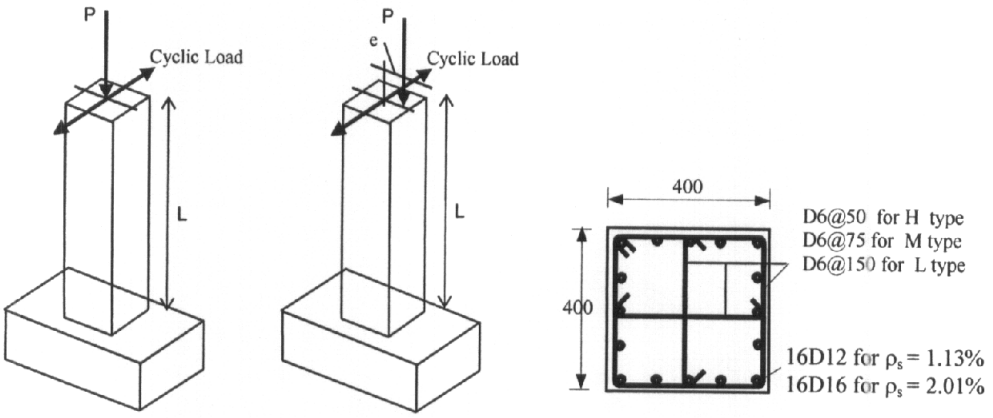

a) Bridge pier model

b) Cross section

Figure 95 Bridge pier specimen models

Table 8 Analytical model specimens

Specimen Type	Tie bar Ratio (ρ_s)	Axial Force Index : (P/f'_cA_g)	Height L (m)	Shear Span Ratio : (L/h)	Axial bar ratio (ρ_l)	Eccentric Load (e/d)
HH31	0.56	0.2	1.4	3.5	1.13	0
HH32	0.56	0.2	1.4	3.5	2.01	0
HH34	0.56	0.2	1.4	3.5	2.01	0.2
HH35	0.56	0.2	1.4	3.5	2.01	0.3
HH36	0.56	0.2	1.4	3.5	2.01	0.4
HM21	0.56	0.12	1.0	2.5	1.13	0
HM31	0.56	0.12	1.4	3.5	1.13	0
HM41	0.56	0.12	1.8	4.5	1.13	0
HM32	0.56	0.12	1.4	3.5	2.01	0
HM33	0.56	0.12	1.4	3.5	2.01	0.2
HM34	0.56	0.12	1.4	3.5	2.01	0.3
HM35	0.56	0.12	1.4	3.5	2.01	0.4
HM36	0.56	0.12	1.4	3.5	1.13	0.2
HM37	0.56	0.12	1.4	3.5	1.13	0.3
HM38	0.56	0.12	1.4	3.5	1.13	0.4
HL31	0.56	0.05	1.4	3.5	1.13	0
HL32	0.56	0.05	1.4	3.5	2.01	0
MH31	0.37	0.2	1.4	3.5	1.13	0
MH32	0.37	0.2	1.4	3.5	2.01	0
MH34	0.37	0.2	1.4	3.5	2.01	0.2
MH35	0.37	0.2	1.4	3.5	2.01	0.3
MH36	0.37	0.2	1.4	3.5	2.01	0.4
MM21	0.37	0.12	1.0	2.5	1.13	0
MM31	0.37	0.12	1.4	3.5	1.13	0
MM32	0.37	0.12	1.4	3.5	2.01	0
MM36	0.37	0.12	1.4	3.5	1.13	0.2
MM37	0.37	0.12	1.4	3.5	1.13	0.3
MM38	0.37	0.12	1.4	3.5	1.13	0.4

Table 8 (Continued)

Specimen Type	Tie bar Ratio (ρ_v)	Axial Force Index : (P/f'_cA_g)	Height L (m)	Shear Span Ratio : (L/h)	Axial bar ratio (ρ_l)	Eccentric Load (e/d)
ML31	0.37	0.05	1.4	3.5	1.13	0
MM41	0.37	0.12	1.8	4.5	1.13	0
ML32	0.37	0.05	1.4	3.5	2.01	0
LL31	0.19	0.05	1.4	3.5	1.13	0
LL32	0.19	0.05	1.4	3.5	2.01	0
LM31	0.19	0.12	1.4	3.5	1.13	0
LM32	0.19	0.12	1.4	3.5	2.01	0
LM21	0.19	0.12	1.0	2.5	1.13	0
LH31	0.19	0.2	1.4	3.5	1.13	0
LM41	0.19	0.12	1.8	4.5	1.13	0
LH32	0.19	0.2	1.4	3.5	2.01	0
LM36	0.19	0.12	1.4	3.5	1.13	0.2
LM37	0.19	0.12	1.4	3.5	1.13	0.3
LM38	0.19	0.12	1.4	3.5	1.13	0.4

All specimens simulating cantilever bridge pier columns shown in Fig. 95 were analyzed. The columns have the same cross section 400 mm × 400 mm and the concrete compressive strength is 28 MPa. The longitudinal reinforcement was deformed bars of diameters 12 mm or 16 mm and diameters 6 mm for tie reinforcements. The yield strength of all the reinforcement was 395 MPa (SD40 grade). The core cross section dimensions are 340 × 340 mm and the bound concrete cover is 30 mm. The tie reinforcement ratios (ρ_v, A_{sh}/sh_c) for this section calculated for seismic design required by AASHTO and ACI as (Equation (1) and (2)) are 0.85% and 0.81 % respectively. The parameters were investigated following:

a) Tie reinforcement ratio, (ρ_v, A_{sh}/sh_c) are 0.19% (L), 0.37% (M) and 0.56% (H) with deformed bar having yield strength 390 MPa (SD40 grade). Based on ASSHTO code, these ratios

correspond to the minimum requirement with non-seismic performance for 0.19% (L) and with 40% and 66% of minimum requirement with seismic performance for 0.37% (M) and 0.56% (H) ratio respectively.

b) Axial load levels are relatively low axial loads for pier columns which are $0.05f_c'A_g$ (224 kN), $0.12f_c'A_g$ (537 kN) and $0.2f_c'A_g$ (896 kN) and the eccentricities (e/h) are 0.2, 0.3 and 0.4.

c) Effective pier heights (l) measured from bottom to the applied loading point are 1.0, 1.4 and 1.8 m. in order to vary the shear span to length ratio (L/h) being 2.5, 3.5 and 4.5.

d) The vertical reinforcement ratios were 1.13% and 2.01% respectively.

The lateral cyclic load was applied at the top of piers by controlling the displacements step wisely from 1% drift ratio (ratio of horizontal displacement to column length) until failure with an increment of 0.5% drift ratio. The number of unloading and reloading was 3 cycles in each increment step as shown in Fig. 96.

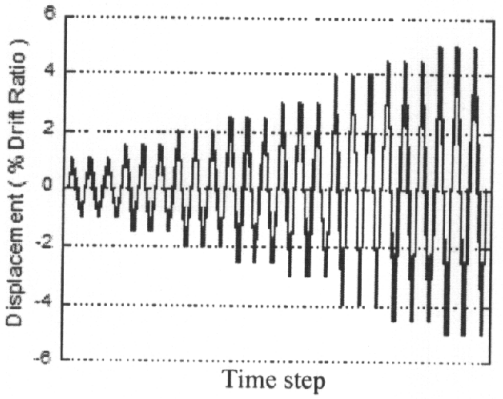

Figure 96 Step-wise increasing of applied displacement loading

Analysis Method

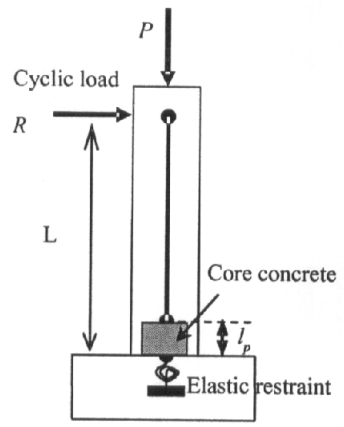

Figure 97 Analytical model

The cantilever column for the analysis was modelled as shown in Fig. 97. The member consisted of a beam element and a confined concrete segment. Towards the maximum lateral load, the confined segment developed a plastic hinge. The plastic hinge zone with length (l_p) calculated based on Paulay, T. and M.J.N. Priestley, 1992 was idealized by a confined fiber element given by Equation (43)

$$l_p = 0.08L + 0.022 d_b f_y \tag{43}$$

Inelastic material properties were considered for the analysis. The stress and strain response was analyzed by the TDAP III program (ARK, Inc., 2000). The rotation spring at the bottom of the column was defined to accommodate the deformation of axial reinforcement. The stress vs. strain function of confined concrete was based on Hoshikuma et al. (1997) as given by Equation (44) and Fig. 98.

$$f_c = \begin{cases} E_c \varepsilon_c \left\{ 1 - \frac{1}{n} \left(\frac{\varepsilon_c}{\varepsilon_{cc}} \right)^{n-1} \right\} & \cdots\cdots 0 \le \varepsilon_c \le \varepsilon_{cc} \\ f_{cc} - E_{des} \left(\varepsilon_c - \varepsilon_{cc} \right) & \cdots\cdots \varepsilon_{cc} < \varepsilon_c \le \varepsilon_{cu} \end{cases} \tag{44}$$

$$n = \frac{E_c \varepsilon_{cc}}{E_c \varepsilon_{cc} - f_{cc}}$$

$$f_{cc} = f_{co} + 0.76 f_{yh}$$

$$\varepsilon_{cc} = 0.002 + 0.0132 \frac{\rho_s f_{yh}}{f_{co}}$$

$$E_{des} = 11.2 \frac{f_{ck}^2}{\rho_s f_{sy}}$$

$$\varepsilon_{cu} = \varepsilon_{cc} + \frac{0.8 f_{cc}}{E_{des}}$$

$$\varepsilon_{cc} = 0.00245 + 0.0122 \frac{\rho_s f_{yh}}{f_{co}}$$

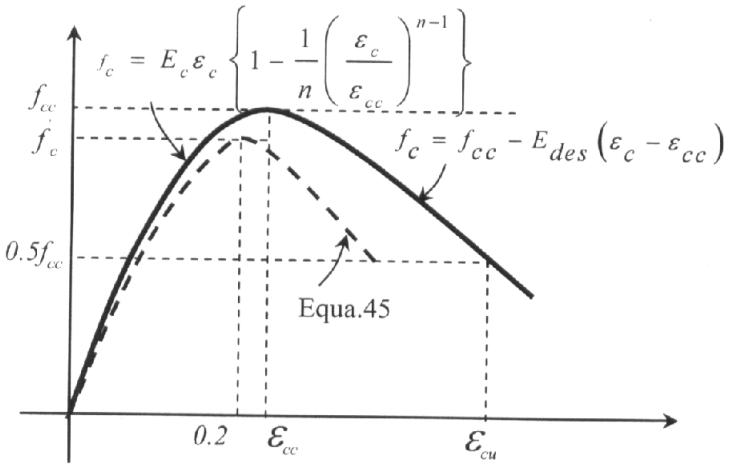

Figure 98 Stress vs. strain curve for confined concrete

For the covering concrete, the stress vs. strain model of the unconfined concrete was idealized as Equation (45).

$$f_c = \begin{cases} E_c \varepsilon_c \left\{ 1 - \frac{1}{n} \left(\frac{\varepsilon_c}{0.002} \right)^{n-1} \right\} & \cdots\cdots 0 \le \varepsilon_c \le 0.002 \\ \frac{f_{cc}}{0.005} (0.007 - \varepsilon_c) & \cdots\cdots 0.002 < \varepsilon_c \le \varepsilon_{cu} \\ 0 & \cdots\cdots \varepsilon_{cu} < \varepsilon_c \end{cases} \qquad (45)$$

The stress vs. strain model of the vertical reinforcement was idealized based on Menegotto. M. and Pinto, P.E. (1973) given by the following non-linear Equation (69) and shown in Fig. 105

$$\tilde{\sigma} = R_s \tilde{\varepsilon} + \frac{(1 - R_s)\tilde{\varepsilon}}{\left(1 + \tilde{\varepsilon}^R\right)^{1/R}} \tag{46}$$

$$\tilde{\sigma} = \frac{\sigma_s - \sigma_r}{\sigma_o - \sigma_r}$$

$$\tilde{\varepsilon} = \frac{\varepsilon_s - \varepsilon_r}{\varepsilon_o - \varepsilon_r}$$

Where the effective strain and stress $(\tilde{\sigma}, \tilde{\varepsilon})$ are a function of the unloading and reloading interval, ε_r, σ_r are the strain and stress at reversal point, ε_o, σ_o are the strain and stress at intersection of the asymptotes, R_s is the ratio of the initial to final tangent stiffness and R is a parameter that defines the shape of unloading curve.

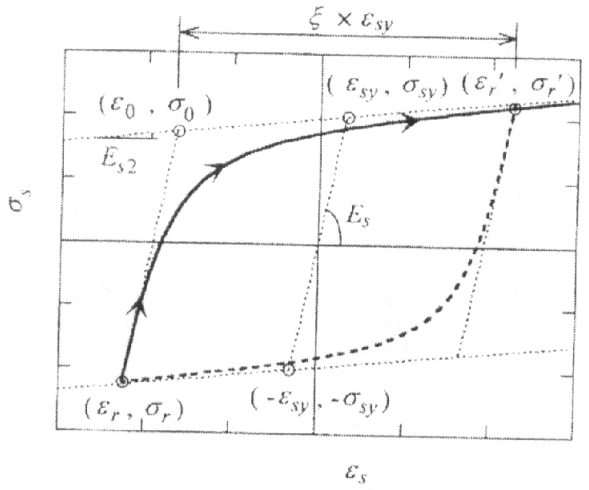

Figure 99 Stress strain curve for vertical steel reinforcement

Source: Menegotto and Pinto (1973)

Analytical Result

The analytical results are shown and compared by envelope curve of the relationship of the compressive stress in the core concrete versus lateral displacement at load point in terms of drift ratio illustrated in Fig. 100. The peak stress of core concrete, f_{cc} and unloading curve depend on the amount of confinement of the core. At first yield of vertical reinforcement, the lateral yielding displacement Δ_y was defined and the corresponding load in R_y. According to Hoshikuma et al. (1997) criteria when the compressive stress dropped below 50% of the peak stress of core concrete, f_{cc} the crushing of core concrete and bucking of longitudinal reinforcement occurred. The corresponding displacement at core failure is defined, Δ_u.

The strength of the column is the maximum lateral load, R_u and the maximum moment is the product of maximum lateral load and the effective height. According to Wehbe et al. (1999) the ultimate drift is defined on the drift at 0.75 of the maximum strength, R_{max}.

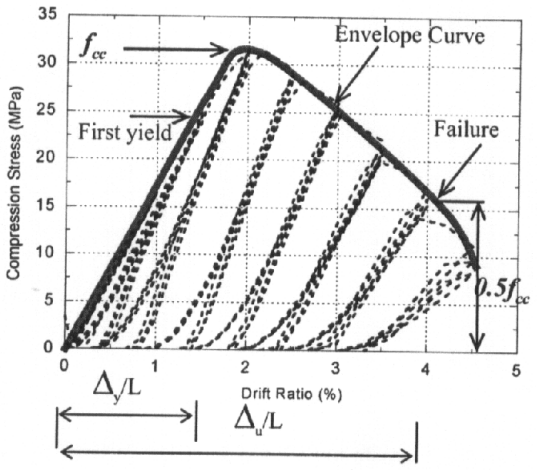

Figure 100 Envelope curve of stress and drift ratio in core concrete

Forty two column models were analysed and Table 5.2 shows the results of drift ratio, Δ_y/L, Δ_u/L, the ductility ratio, Δ_u/Δ_y, the yielding moment and maximum moment at yield of

axial reinforcement and at failure, ductility and maximum moment. The drift ratio was calculated as the ratio of displacement and effective height.

The comparison of the envelope curves for clearing the parameters are shown as follow.

Table 9 Analytical results

Type	$\frac{100\Delta_y}{L}(\%)$	$\frac{100\Delta_u}{L}(\%)$	$\mu=\frac{\Delta_u}{\Delta_y}$	M_y (kN-m)	M_{max} (kN-m)
HH31	1.03	3.22	3.13	218.3	246.53
HH32	1.29	3.42	2.65	281.45	322.78
HH34	1.00	2.00	2	282.12	308.45
HH35	0.93	1.50	1.61	263.75	286.02
HH36	0.80	1.50	1.88	228.7	261.17
HM21	0.72	3.38	4.69	178.58	213.69
HM31	0.85	4.00	4.71	175.8	212.04
HM41	0.99	4.61	4.66	174.42	209.34
HM32	1.10	4.11	3.74	238.53	297.08
HM33	1.00	2.81	2.81	267.68	288.49
HM34	0.93	2.68	2.88	255.76	280.61
HM35	0.87	2.31	2.66	240.89	268.01
HM36	0.73	2.51	3.44	185.99	202.88
HM37	0.67	3.00	4.48	173.19	196.04
HM38	0.60	2.50	4.17	157.71	186.46
HL31	0.67	5.25	7.84	172.5	176.55
HL32	0.94	4.62	4.91	200.51	266.61
MH31	1.03	2.53	2.46	217.25	248.55
MH32	1.29	2.74	2.12	282.1	324.91
MH34	1.10	2.27	2.06	302.81	322.21

Table 9 (Continued)

Type	$\frac{100\Delta_y}{L}(\%)$	$\frac{100\Delta_u}{L}(\%)$	$\mu=\frac{\Delta_u}{\Delta_y}$	M_y (kN-m)	M_{max} (kN-m)
MH35	1.10	2.20	2	291.37	314.38
MH36	1.00	2.09	2.09	280.03	203.73
MM21	0.72	2.60	3.61	178.75	214.87
MM31	0.85	3.07	3.61	175.98	213.11
MM32	1.10	3.25	2.95	238.84	294.41
MM36	0.73	2.06	2.82	186.42	203.73
MM37	0.67	1.50	2.24	173.72	197
MM38	0.60	1.00	1.67	158.24	187.67
MM41	0.99	3.60	3.64	174.6	210.13
ML31	0.67	3.95	5.9	171.8	176.55
ML32	0.94	3.82	4.06	200.72	264.27
LL31	0.67	2.83	4.22	171.51	177.51
LL32	0.94	2.82	3	201.02	264.13
LM31	0.85	2.24	2.64	176.77	214.44
LM32	1.10	2.39	2.17	237.17	295.16
LM21	0.72	1.90	2.64	181.93	216.16
LH31	1.03	1.81	1.76	217.87	250.82
LM41	0.99	2.52	2.55	176.87	211.03
LH32	1.29	2.06	1.6	283.6	325.91
LM36	0.73	1.53	2.1	186.96	204.69
LM37	0.67	1.33	1.99	174.39	198.24
LM38	0.60	1.00	1.67	158.97	188.63

Comparison of Compressive Stress in Core Concrete and Drift Ratio

Fig. 101 shows the lateral force and drift ratio hytereses of specimens HL31 MM31 and LM 31.

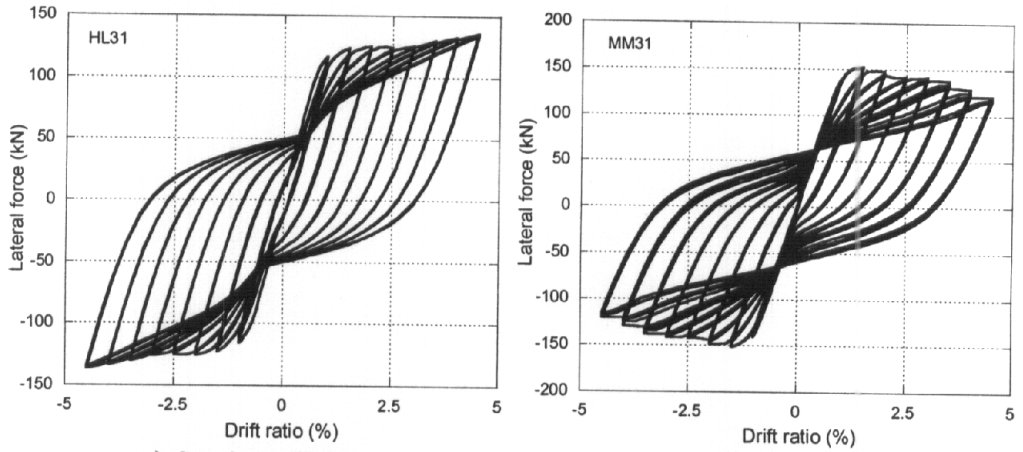

a) Specimen HL31

b) Specimen MM31

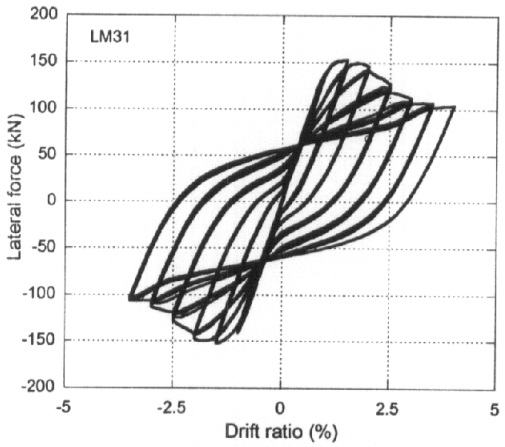

c) Specimen LL31

Figure 101 Lateral force vs. drift ratio hytereses from analytical studies of analyzed specimens

To compare the strength and ductility of columns, the relationship of compressive stress of core concrete and drift ratio for the support length is considered as shown in Fig. 102 through Fig 104.

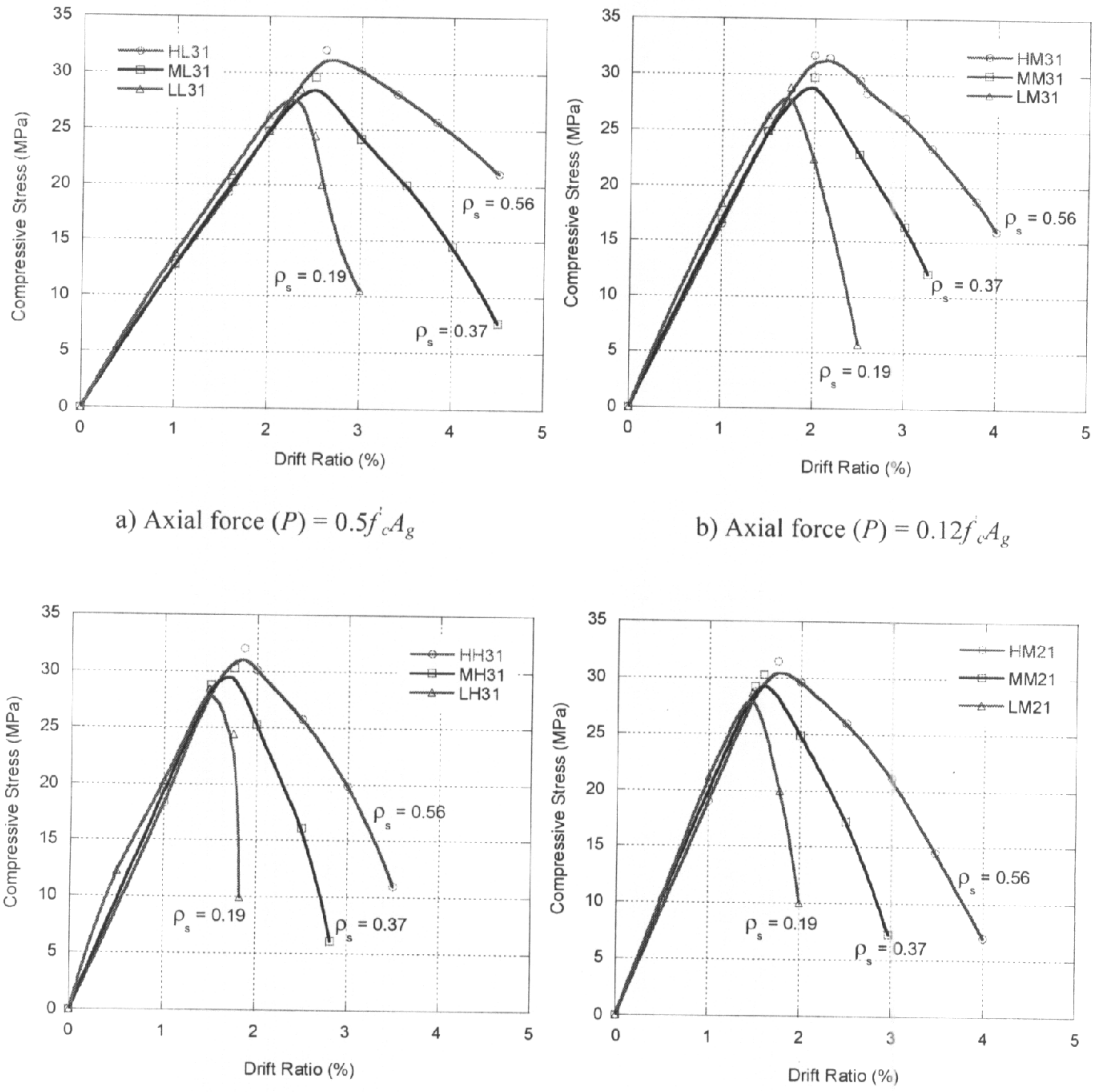

a) Axial force $(P) = 0.5f'_cA_g$

b) Axial force $(P) = 0.12f'_cA_g$

c) Axial force $(P) = 0.2f'_cA_g$

d) Shears span ratio $(l/h) = 2.5$

Figure 102 Compressive stress and drift ratio in core concrete

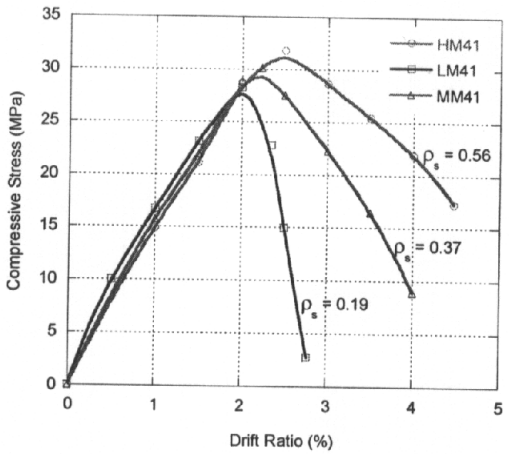

e) Shear Span Ratio (l/h) = 4.5

Figure 102 (Continued)

The effect of tie reinforcement ratio of specimens with axial reinforcement ratio (ρ_s) 1.13 % under constant axial load (P) varied from $0.05f'_cA_g$, $0.12f'_cA_g$ and $0.2f'_cA_g$ are shown in Fig. 102a, 102b and 102c respectively. The shear span ratio (l/h) varied between 2.5 3.5 and 4.5 are shown in Fig. 103.

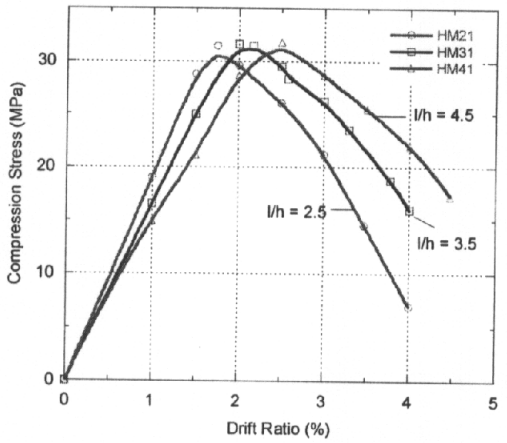

Figure 103 Envelope curve of compressive stress and drift ratio in core concrete (varying shear span ratio)

Fig. 103 shows the effect of shear span ratio (l/h) varying 2.5, 3.5 and 4.5 with axial reinforcement ratio (ρ_l) = 1.13 and $P = 0.12f'_cA_g$.

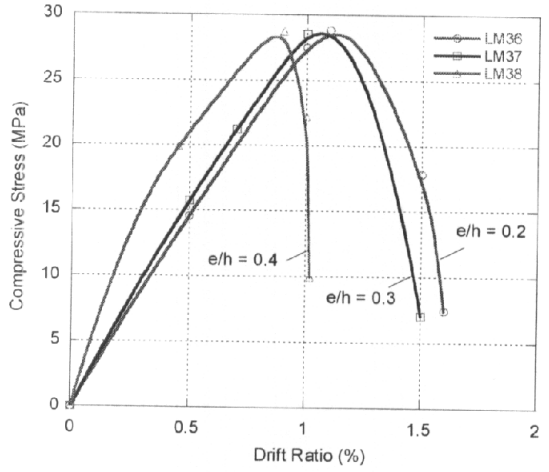

a) Tie reinforcement ratio (ρ_s) = 0.19%

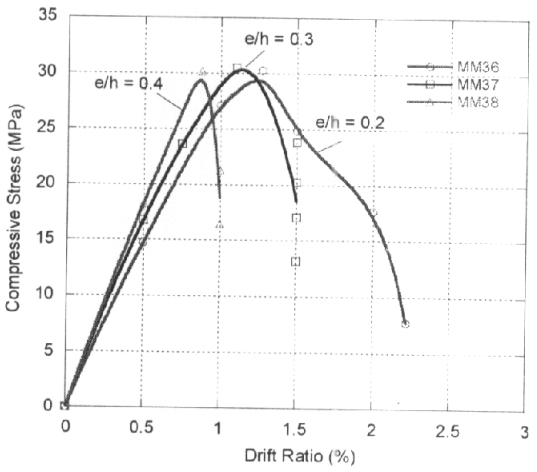

b) Tie reinforcement ratio (ρ_s) = 0.37%

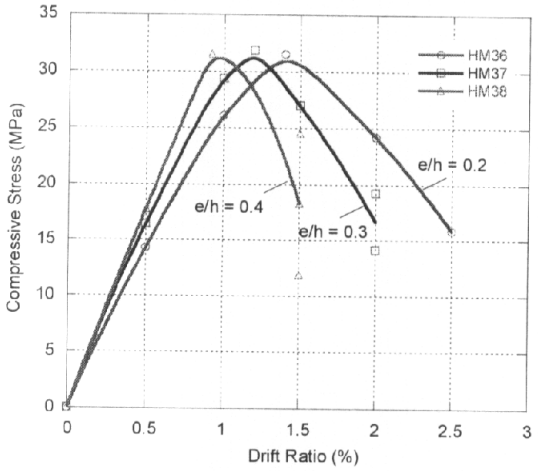

c) Tie reinforcement ratio (ρ_s) = 0.56%

Figure 104 Compressive stress and drift ratio in core concrete

For the effect of eccentric loading (*e/h*) of constant axial load varying 0.2, 0.3 and 0.4 with axial reinforcement ratio (ρ_l): 1.13 was shown in Fig. 104 a, b and c respectively.

The lateral force vs. displacement from analytical are shown in Appendix Fig. 10 and the stress vs. strain data of core concrete from analytical and Appendix Fig. 11.

Comparison of Ductility

The ductility factor is defined by the ratio of the displacement at failure (Δ_u) and at yield of longitudinal steel bars (Δ_y) illustrated in Fig. 105.

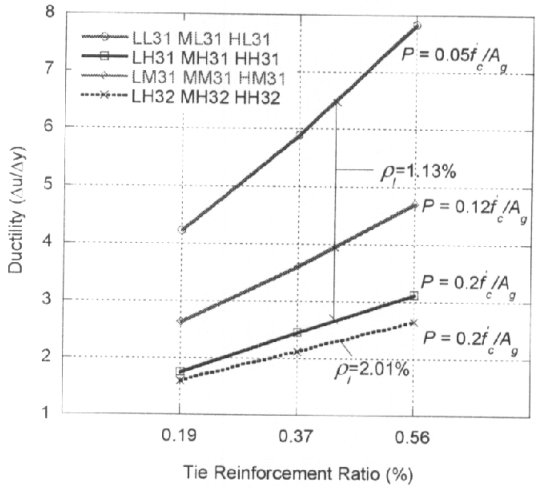

a) Axial reinforcement ratio (ρ_l) = 1.13%

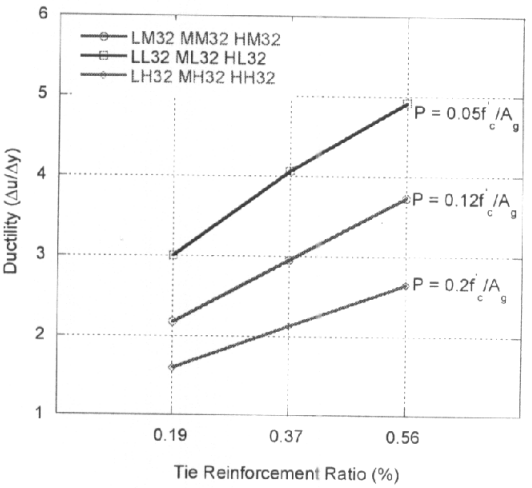

b) Axial reinforcement ratio (ρ_l) = 2.01%

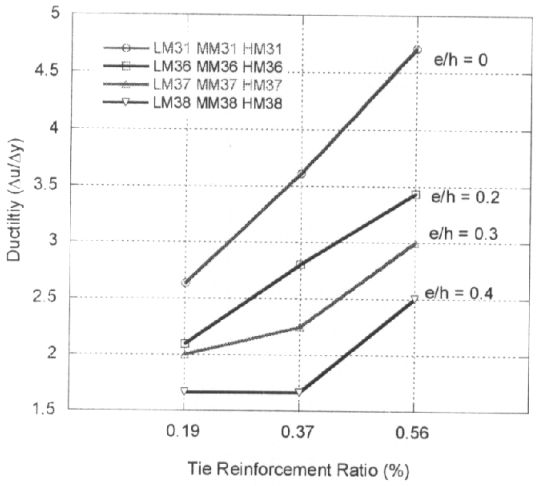

c) Axial reinforcement ratio (ρ_l) = 1.13% and axial force (P) = $0.12 f'_c A_g$

Figure 105 Ductility factor and tie reinforcement ratio

Fig 105 a. and 105 b. show comparison of the ductility factor for the columns varying the axial force, $P = 0.05 f'_c A_g$, $0.12 f'_c A_g$ and $0.2 f'_c A_g$ respectively.

Comparison of Strength

The strength is defined by the maximum moment capacity calculated by the maximum moment at the support length, l_p of column. Fig. 107 shows the maximum moment capacity versus the constant axial load with varying eccentricity loading and axial force level respectively.

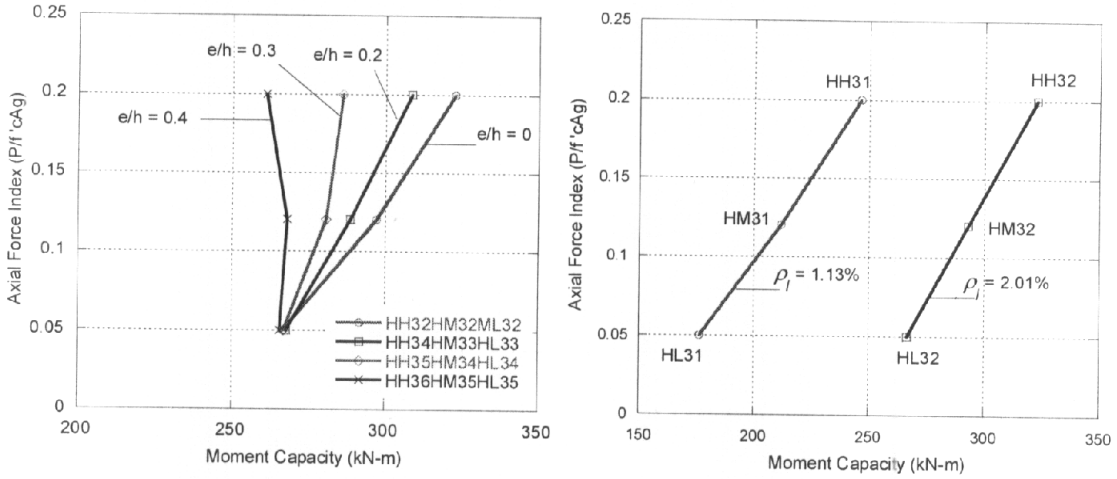

a) Eccentric loading (e/h) varying from 0 to 0.4 b) Axial reinforcement ratio (ρ_l) varied = 1.13% and 2.01%

Figure 106 Comparison of axial force index and moment capacity

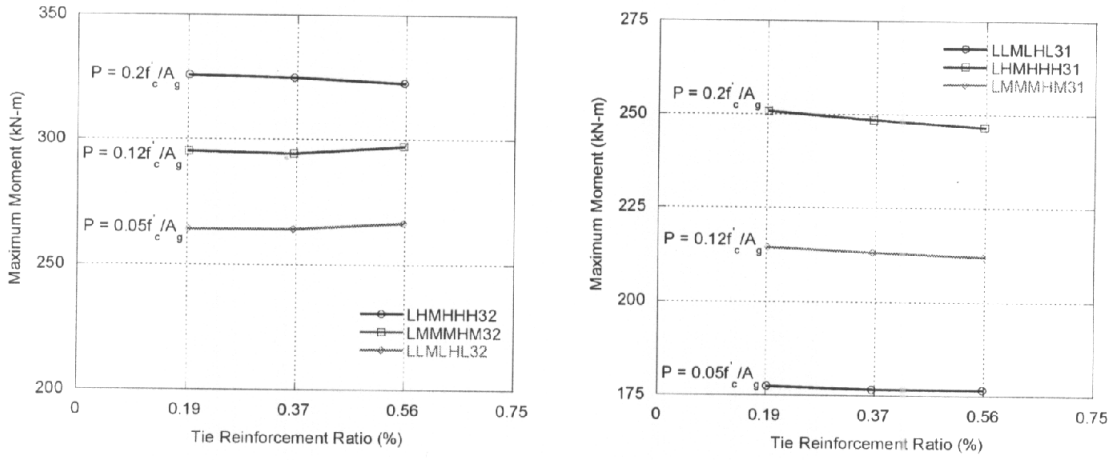

Figure 107 Comparison of moment capacity and tie reinforcement ratio

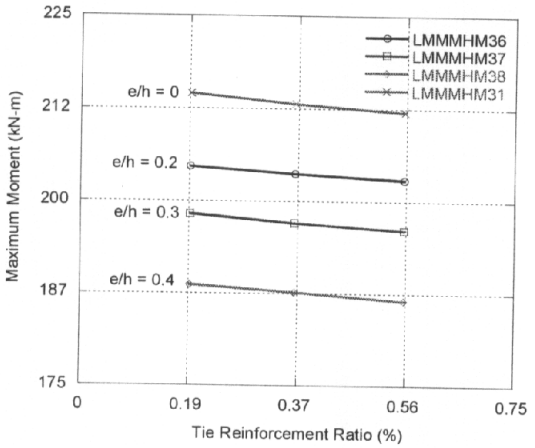

Figure 107 (Continued)

Discussion on Analytical Study

The failure mode of all specimens subjected low constant axial load level in the tension controlled zone ($0.05 f_c' A_g$, $0.12 f_c' A_g$ and $0.2 f_c' A_g$) and bending due to cyclic loading can be computed to determine the effects of parameters on the response behavior of columns as follow:

Effect of the Tie bar Ratio

1. The compressive strength of core concrete and ductility are increased significantly relating to increases in amount of the tie reinforcement as shown in Fig. 102
2. The descending branch of compressive stress of core concretes dropped more rapidly with decreased tie reinforcement ratio.

Effect of the Shear Span Ratio

1. The maximum drift ratio decreased with increasing the shear span ratio as shown in Fig. 103.
2. The ascending branch of compressive stress of core concrete increases more rapidly with lower shear span ratio as shown in Fig. 103.

Effect of Axial Force and eccentricity

1. The ductility capacity decreases significantly as the applied higher axial load as shown in Fig. 105 a and 105 b.
2. Within low axial loading and tension zone failure, the maximum moment capacity increases when higher axial load as shown in Fig. 106 b.
3. The ductility in descending branch is decrease when eccentricity was large as shown in Fig. 104.
4. When the eccentric loading was applied approximately with *e/h* more than 0.2, the ductility factor was decreased rapidly as shown n Fig. 105 c.

Effect of the Axial Bar Ratio

1. The axial bar ratio increased from 1.13% to 2.01 % affect to decrease the ductility capacity as shown in Fig. 105a.
2. Yielding moment capacity increase when increased axial bar.

Discussion

From analytical results shown in Fig. 101a, the lateral force beyond the peak load does not unload for the specimens with high confining reinforcement whiles the specimens with low confining reinforcement unloads. This is the due to the fact that the failure criterion of condition the ultimate strain at 75% of R_{max} is not accurately predicted. The effect of local buckling and rupture of vertical reinforcements is not included in the fiber element analysis.

Considering Appendix Fig. 8d and Appendix Fig. 9d, it was found that the ultimate strain in ties bar for specimen D1 measured at drift ratio 4.5% if 950×10^{-6}. This corresponds to axial strain of 0.006 corresponding with the axial strain at 50% of peak stress based on Hoshikuma et al. (1997) being 0.0045. The failure criterion when the compressive stress dropped below 50% of peak stress of core concrete is good agreement.

The axial force level significantly affects ductility of columns. The levels of confinement provided by tie reinforcement depend on the axial force level. Considering Fig. 105a, at axial force level of $0.2f_c^{'}/A_g$ the provided tie reinforcement ratio, ρ_s is not less than 0.6 giving the ductility ratio of 3. For axial force level of $0.12f_c^{'}/A_g$, ρ_s is not less than 0.3 giving the ductility ratio of 3.

For the columns provided by tie reinforcement ratio, ρ_s less than 0.19 corresponding to the required AASHTO non-seismic giving low ductility ranging between 1and 3.